

Specificity and Affinity of Natural Product Cyclopentapeptide Inhibitors against *A. fumigatus*, Human, and Bacterial Chitinases

Francesco V. Rao,¹ Douglas R. Houston,¹
Rolf G. Boot,² Johannes M.F.G. Aerts,²
Michael Hodgkinson,¹ David J. Adams,³
Kazuro Shiomi,⁴ Satoshi Ōmura,^{4,5}
and Daan M.F. van Aalten^{1,*}

¹Division of Biological Chemistry & Molecular Microbiology

School of Life Sciences
University of Dundee

Dundee DD1 5EH, Scotland

²University of Amsterdam

Academic Medical Center
Department of Medical Biochemistry
1105 AZ, Amsterdam

The Netherlands

³School of Biochemistry and Microbiology
University of Leeds

Leeds LS2 9JT

United Kingdom

⁴School of Pharmaceutical Sciences and

⁵Kitasato Institute for Life Sciences

Kitasato University

The Kitasato Institute

Minato-ku, Tokyo 108-8641

Japan

Summary

Family 18 chitinases play key roles in organisms ranging from bacteria to man. There is a need for specific, potent inhibitors to probe the function of these chitinases in different organisms. Such molecules could also provide leads for the development of chemotherapeutics with fungicidal, insecticidal, or anti-inflammatory potential. Recently, two natural product peptides, argifin and argadin, have been characterized, which structurally mimic chitinase-chitooligosaccharide interactions and inhibit a bacterial chitinase in the nM–mM range. Here, we show that these inhibitors also act on human and *Aspergillus fumigatus* chitinases. The structures of these enzymes in complex with argifin and argadin, together with mutagenesis, fluorescence, and enzymology, reveal that subtle changes in the binding site dramatically affect affinity and selectivity. The data show that it may be possible to develop specific chitinase inhibitors based on the argifin/argadin scaffolds.

Introduction

Family 18 chitinases (CAZY GH 18 [<http://afmb.cnrs-mrs.fr/CAZY>]) hydrolyze chitin, a homopolymer of N-acetylglucosamine. They are found in organisms ranging from bacteria (e.g., [1]) to mammals [2, 3], where they have diverse functions ranging from accessing chitin as an energy resource to pathogen defense. Recent reports have highlighted the interest in chitinase inhibitors as

molecules with chemotherapeutic potential against pathogenic fungi [4], insects [5, 6], malaria transmission [7–9], and human asthma [10]. Several different classes of chitinase inhibitors have been reported. Allosamidin, a pseudotrisaccharide isolated from *Streptomyces*, is the most characterized of these and inhibits family 18 chitinases in the nM range [11, 12]. A wealth of structural information is available demonstrating how this natural product binds to family 18 chitinases [13–17]. Unfortunately, allosamidin is no longer commercially available and total synthesis is complicated [18]. Cyclic proline-containing dipeptides have also been reported as chitinase inhibitors, although the most potent of these currently only inhibit in the high μ M range [19–22].

Recently, a novel class of natural product chitinase inhibitors has been reported. Two cyclic pentapeptides, argifin [5] and argadin [6] (Figure 1), were isolated from *Gliocladium* and *Clonostachys* fungal cultures, respectively. Initial tests against an insect chitinase from the blowfly *Lucilia cuprina* revealed that argifin and argadin inhibited the enzyme with surprisingly low IC_{50} values in the nanomolar range, respectively [5, 6]. A subsequent structural study revealed the binding mode of argifin and argadin to chitinase B of the soil bacterium *Serratia marcescens*, showing that these peptides precisely mimicked the interaction between substrate (i.e., chitin/chitooligosaccharides) and the protein. Argifin/argadin appeared to occupy sugar subsites –1, +1, +2 (standard glycosidase nomenclature, with the scissile bond between the –1 and +1 subsites [23]), whereas allosamidin binds to the –3, –2, –1 subsites [13–16]. *Serratia marcescens* chitinase B (*SmChiB*) belongs to a subclass of chitinases known as the “bacterial” class of chitinases [4, 24] which, apart from a catalytic core based on a $(\beta\alpha)_8$ fold, contain a separate α/β domain that gives the active site a deep, almost tunnel-like character [14, 25] toward the +1, +2 subsites. In contrast, chitinases of the “plant” class (e.g., hevamine from *Hevea brasiliensis* [13]) contain the $(\beta\alpha)_8$ catalytic core only, with a fully exposed active site and no well-defined +1, +2 subsites.

The opportunistic fungal pathogen *Aspergillus fumigatus* produces a wide range of chitinolytic enzymes including family 18 chitinases of both the bacterial and plant classes. The secreted *ChiB1* chitinase (*AfChiB1*) is the major, inducible member of the former class [26], and in this study we investigate the effects of argifin and argadin on *AfChiB1* and a human bacterial-class chitinase (chitotriosidase; HCHT). Our aim is to determine whether these cyclopentapeptides or their derivatives are suitable scaffolds for further optimization to selectively inhibit specific target chitinases. A combination of X-ray crystallography, mutagenesis, enzymology, and ligand binding studies is used to probe the key contributions and differences in binding in context of high-resolution crystal structures of the *AfChiB1*/HCHT argifin/argadin complexes. Despite high sequence conservation in the vicinity of the active site, affinity for argifin/argadin differs significantly between

*Correspondence: dava@davapc1.bioch.dundee.ac.uk

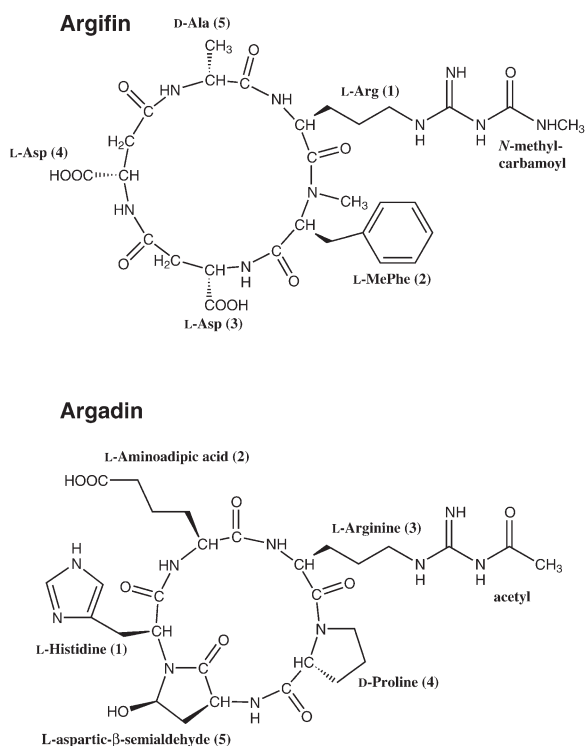


Figure 1. Chemical Structures of Argifin and Argadin

The 2D chemical structures, with configuration of stereocenters as defined through a combination of spectroscopic analyses [5, 6] and X-ray crystallography [37], are shown. The individual amino acid moieties are numbered to allow crossreferencing with Table 1.

these chitinases and could be exploited for the design of specific argifin/argadin derivatives in the future.

Results

AfChiB1 Structure

The major secreted chitinase of *Aspergillus fumigatus*, AfChiB1, was cloned and overexpressed as a GST fusion protein in *E. coli*. Following purification and cleavage of the GST, full-length AfChiB1 was crystallized using Li_2SO_4 solutions. Synchrotron diffraction data collected to 1.7 Å resolution (see Supplemental Table S1) were used to solve the structure by molecular replacement, followed by refinement, which yielded a final model with an R factor of 0.180 ($R_{\text{free}} = 0.200$) (Table S1). The AfChiB1 structure represents the second example of a fungal chitinase structure, the first one being CTS1 from *Coccidioides immitis* (CiCTS1), for which both an unliganded structure and an inhibitor complex with allosamidin have been determined [15, 27]. AfChiB1 is 66% identical in sequence to CiCTS1, with no insertions or deletions. The structures are similar, with an rmsd of 0.7 Å on $\text{C}\alpha$ atoms. AfChiB1 contains a $(\beta\alpha)_8$ fold but lacks helix $\alpha 1$ (Figure 2), in common with other proteins from the family 18 chitinase family [27–29]. Asp175 and Glu177 at the end of $\beta 4$ form part of the family 18 chitinase DxE motif (see CAZY [<http://afmb.cnrs-mrs.fr/CAZY>]), with Glu177 as the catalytic

acid. A path of solvent-exposed aromatic residues runs through the active-site cleft (Figure 2). Mutagenesis and crystallographic studies have shown that these side chains play a key role in substrate/inhibitor binding [15, 30–32].

Although AfChiB1 was crystallized in the absence of any substrate/inhibitor and was not cryoprotected with organic solvent, well-defined density for a small molecule was found in the active site (Figure 2B). A Tris molecule present in the protein buffer was found to fit this density and was included in further refinement. Tris has five hydrogen bonds to active site residues, all of which, with the exception of Asp246, are conserved in family 18 chitinases. The catalytic acid Glu177, presumably deprotonated, hydrogen bonds the Tris amine and one of the hydroxyls, whereas Tyr245, which is thought to participate in transition-state stabilization [15, 21, 31, 33], hydrogen bonds another hydroxyl (Figure 2B). Although, to our knowledge, this is the first report of Tris binding to a family 18 chitinase active site, Tris has been previously described as binding to and/or inhibiting other glycoside hydrolases [34–36].

Structures of AfChiB1 and HCHT with Argifin and Argadin

Argifin was soaked into AfChiB1 crystals, synchrotron data were collected, and the AfChiB1-argifin complex was refined to 2.0 Å resolution (Table S1). Argifin was also cocrystallized with the human chitotriosidase (HCHT), synchrotron data were collected, and the HCHT-argifin complex was refined to 1.65 Å resolution (Table S1). The AfChiB1-argifin and HCHT-argifin complexes are compared to the published SmChiB-argifin complex [37] in Figure 3, and a quantitative comparison of hydrogen bonding contacts is shown in Table 1. Argifin appears to bind the three different family 18 chitinases through residues that are mostly conserved. The guanyl-urea moiety stacks on a conserved tryptophan (Trp384 in AfChiB1) and interacts with the glutamate and aspartate from the family 18 chitinase DxE motif (Glu177 and Asp175 in AfChiB1, respectively). On the opposite side of the active site, the guanyl-urea moiety also interacts with a conserved tyrosine (Tyr245 in AfChiB1), while only AfChiB1 establishes a significant hydrogen bond from the conserved Asp246. The argifin N-methylphenylalanine is sandwiched between two aromatic residues (Trp137 and Phe251 in AfChiB1). Almost all bacterial-type chitinases have two tryptophans at these positions; however, AfChiB1 unusually has a phenylalanine at position 251. Apart from a further hydrogen bond to a conserved arginine (Arg301 in AfChiB1), there are no other direct hydrogen bonds between the three chitinases and argifin. In SmChiB, only an extended loop (near Asp316) closely packs with argifin, but no favorable interactions are established. While argifin binds to AfChiB1 and HCHT in a similar position and orientation (maximum coordinate shift in argifin backbone after superposition of the AfChiB1 and HCHT proteins is 0.6 Å), it seems to be significantly shifted in the SmChiB complex (maximum coordinate shift in argifin backbone after superposition of the AfChiB1/HCHT and SmChiB proteins is 1.9 Å). Thus, with the exception of AfChiB1 Phe251 and SmChiB

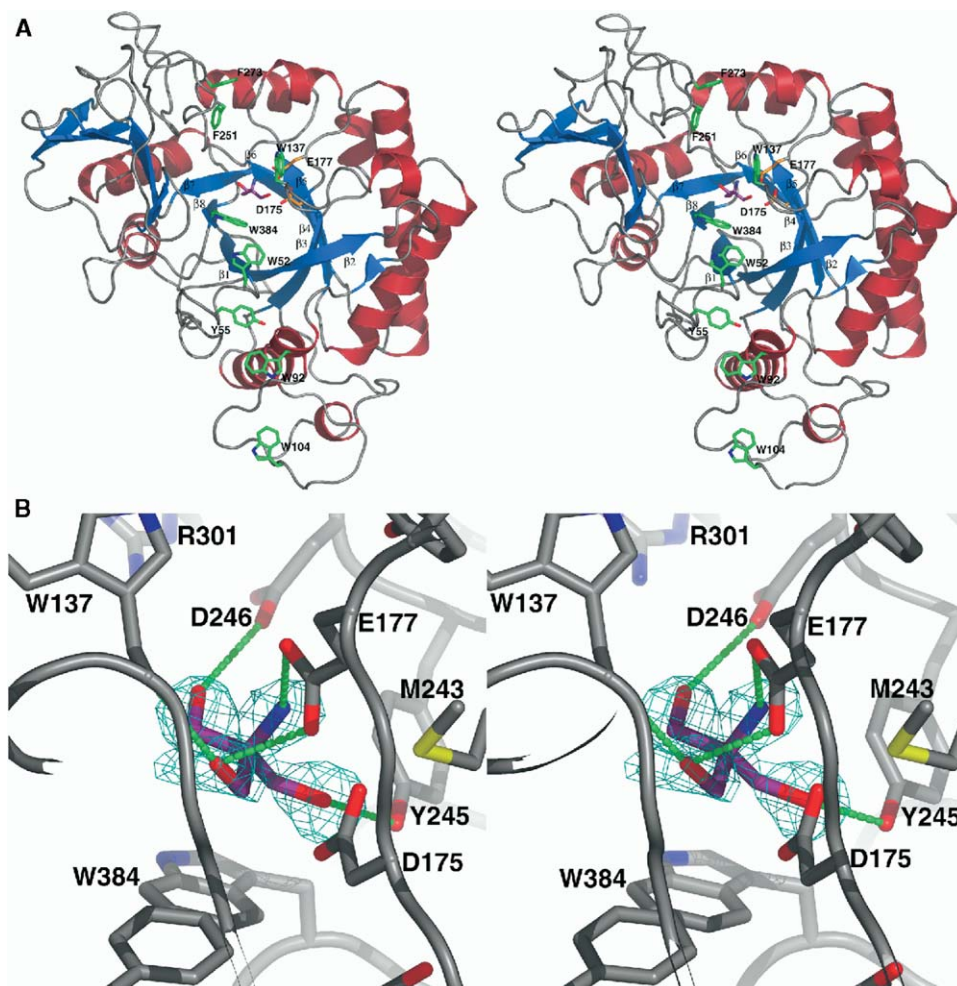


Figure 2. Structure of AfChiB1

(A) Stereo figure of the AfChiB1 fold, shown as a ribbon drawing. Solvent-exposed aromatic residues are shown with green carbon atoms. The Glu177 and Asp175 from the family 18 chitinase DxE motif are shown with orange carbon atoms. The ordered Tris molecule in the active site is shown with magenta carbon atoms.

(B) Stereo figure of the AfChiB1 active site identifying the key residues and showing an unbiased $|F_o| - |F_c|$, ϕ_{calc} electron density map (2.5 σ , cyan) together with a Tris molecule (magenta carbon atoms). Hydrogen bonds between AfChiB1 residues and Tris are shown as green dashed lines.

Asp316, the residues directly contacting argifin are conserved in the three chitinases studied here, although some differential contacts are made through water-mediated hydrogen bonds (Figure 3; Table 1).

Crystal structures of argadin complexed to both AfChiB1 (to 1.85 Å resolution) and HCHT (to 1.75 Å resolution) were also refined (Table S1). The AfChiB1-argadin and HCHT-argadin complexes are compared to the published SmChiB-argadin complex in Figure 4, and a quantitative comparison of hydrogen bonding contacts is shown in Table 1. Argadin binds the three chitinases in a similar orientation and position, although the inhibitor sits somewhat deeper into the active site in the HCHT complex (maximum shift of equivalent atoms in argadin after superposition of the three proteins is 1.1 Å). The cyclized aspartic β -semialdehyde stacks with the same conserved tryptophan (Trp384 in AfChiB1) as the argifin guanyl-urea moiety (Figure 4).

This interaction is reminiscent of the observed stacking with a GlcNAc pyranose in chitinase-substrate complexes [30, 31, 37]. The argadin histidine side chain penetrates the active site to establish contacts with the DxE motif. Intriguingly, the histidine backbone oxygen approaches the catalytic glutamate to within 3 Å resolution (Figure 4). Given the pH of the crystallization buffer and the enzyme assays, these atoms would both be deprotonated, and no hydrogen bond could form. However, Glu177 is the catalytic *acid*, i.e., the residue that protonates the scissile glycosidic bond. It may well be that the pK_a of this residue is tuned by its surroundings so that it is protonated near neutral pH, and thus an additional hydrogen bond may well exist to the argadin histidine backbone oxygen. On the opposite side of the active site, a conserved cluster of residues (Tyr245, Asp246, and Arg301 in AfChiB1) establishes three hydrogen bonds observed in all three chitinase-argadin

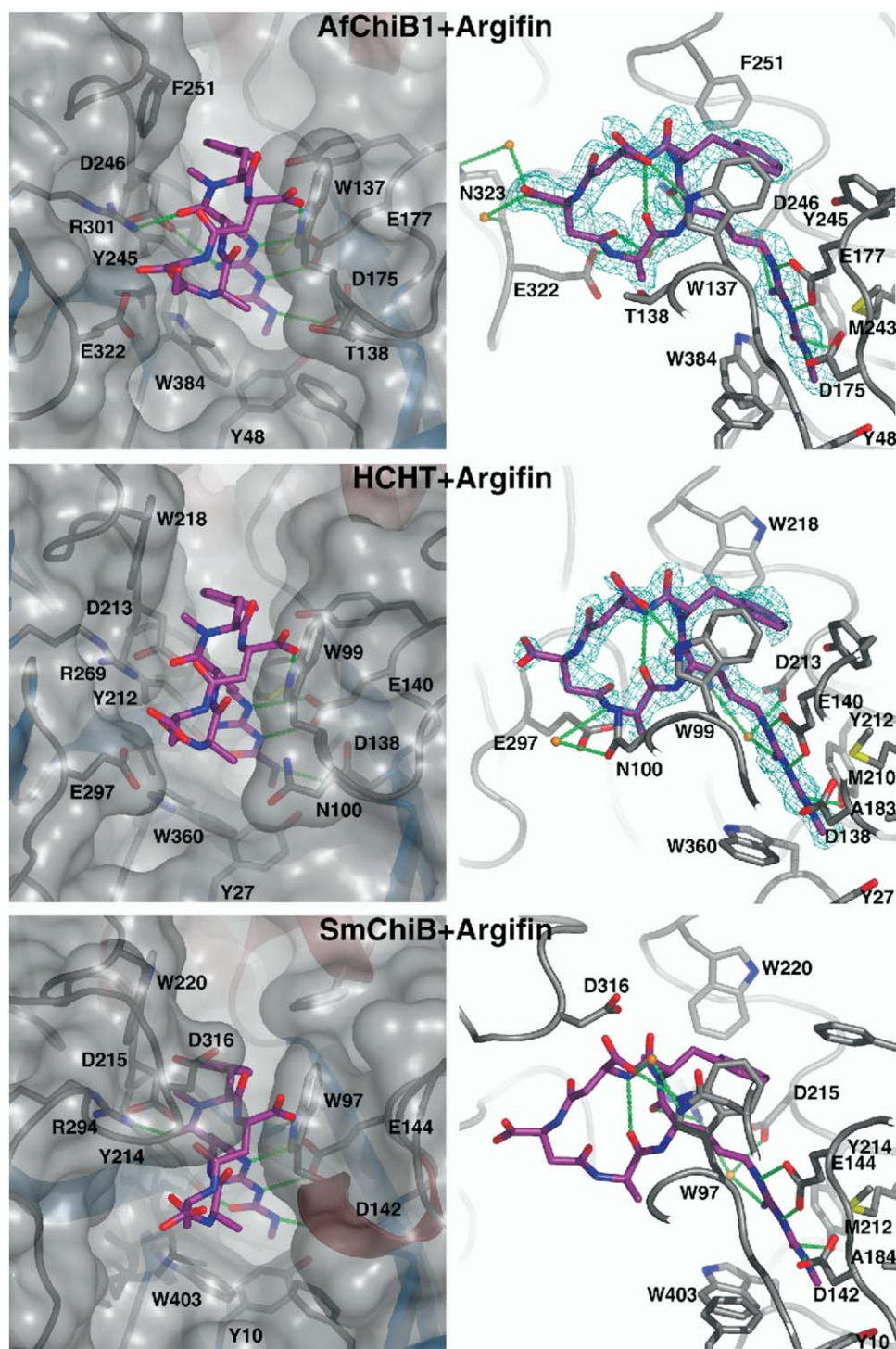


Figure 3. Comparison of Argifin Binding to Family 18 Chitinases

The crystal structures of argifin (magenta carbon atoms) in complex with AfChiB1, HCHT, and SmChiB are shown as a transparent surface (left column) or sticks (right column) representations in two different orientations. Unbiased $|F_o| - |F_c|$, ϕ_{calc} electron density maps, used for building the initial inhibitor models, are shown in cyan, contoured at 2.5σ . Hydrogen bonds with a WHAT IF HB2 score > 0.3 (see Table 1) are shown as green dashed lines. Water molecules involved in water-mediated protein-ligand hydrogen bonds (Table 1) are shown as orange spheres (in the sticks images only). Protein side chains shown are those within a WHAT IF [60] contact distance of 0.75 \AA from the ligand.

complexes (Figure 4; Table 1). Interestingly, in all three complexes, two water molecules are observed at equivalent positions mediating hydrogen bonds be-

tween argifin and the protein backbone (AfChiB1 Trp137 and Asp246). The argifin N^{ω} -acetylarginine and amino adipic acid side chains are aligned side to side

Table 1. Details of Argifin Binding to Family 18 Chitinases

Argifin	AfChiB1	HCHT	SmChiB
Binding/inhibition (μM)	$K_d = 0.46/IC_{50}=1.1$	$IC_{50} = 4.5$	$K_i = 33$
Buried surface (\AA^2)	112	121	133
Internal energy (kJ/mol)	-212	-211	-199
H bonds (protein)			
3,O δ 1	W137,N ϵ 1 (0.80)	W99,N ϵ 1 (0.77)	W97,N ϵ 1 (0.74)
1,O ι 1	Y245,O η (0.66)	Y212,O η (0.72)	Y214,O η (0.72)
1,O	R301,N η 1 (0.16)		
1,O	R301,N η 2 (0.44)		R294,N η 2 (0.31)
1,N ι 2	D175,O δ 2 (0.55)	D138,O δ 2 (0.51)	D142,O δ 2 (0.46)
1,N ι 2	E177,O ϵ 2 (0.37)	E140,O ϵ 2 (0.33)	E144,O ϵ 2 (0.33)
1,N η 1	E177,O ϵ 2 (0.70)	E140,O ϵ 2 (0.62)	E144,O ϵ 2 (0.68)
1,N η 2	D246,O δ 2 (0.53)	D213,O δ 2 (0.23)	
1,N ϵ	E177,O ϵ 1 (0.71)	E140,O ϵ 1 (0.81)	E144,O ϵ 1 (0.67)
H bonds (water)			
3,O δ 1			W1971 (0.68)
4,O δ 1	W2369 (0.77)		
4,O δ 1	W2448 (0.64)		
4,O δ 1	W2677 (0.45)		
4,O	W3067 (0.67)		
1,N η 2	W2085 (0.14)	W48 (0.69)	W1551 (0.73)
5,N		W73 (0.59)	
H bonds (internal)			
1,O ι 1	1,N η 2 (0.54)	1,N η 2 (0.57)	1,N η 2 (0.57)
5,O	3,N (0.70)	3,N (0.78)	3,N (0.75)
Argadin			
Binding/inhibition (μM)	$K_d = 0.81/IC_{50}=0.5$	$IC_{50} = 0.013$	$K_i = 0.020$
Buried surface (\AA^2)	130	138	148
Internal energy (kJ/mol)	-107	-133	-81
H bonds (protein)			
3,O	R301,N η 1 (0.40)	R269,N η 1 (0.27)	
3,O	R301,N η 2 (0.64)	R269,N η 2 (0.54)	R294,N η 2 (0.70)
5,O δ 1	R301,N η 2 (0.29)	R269,N η 2 (0.31)	
5,O δ 1	D246,O δ 2 (0.67)	D213,O δ 2 (0.54)	D215,O δ 2 (0.64)
1,N ϵ 2	D175,O δ 2 (0.73)	D138,O δ 2 (0.78)	D142,O δ 2 (0.77)
1,N δ 1	Y245,O η (0.87)	Y212,O η (0.88)	Y214,O η (0.76)
H bonds (water)			
5,O δ 1			W1131 (0.80)
2,O ζ 1	W2232 (0.77)	W1078 (0.73)	W1502 (0.69)
2,O ζ 1		W1157 (0.58)	
1,O	W2250 (0.32)		
2,O		W1059 (0.59)	
H bonds (internal)			
2,O ζ 1	3,N η 1 (0.69)	3,N η 1 (0.88)	3,N η 1 (0.79)
3,O ι 1	3,N η 2 (0.57)	3,N η 2 (0.57)	3,N η 2 (0.51)
2,O ζ 2	3,N ϵ (0.75)	3,N ϵ (0.94)	3,N ϵ (0.86)
2,O ζ 2	3,N (0.62)	3,N (0.69)	3,N (0.78)
2,O	5,N (0.43)	5,N (0.41)	5,N (0.20)
5,O δ 1	2,N (0.79)	2,N (0.85)	2,N (0.79)

Argifin/argadin internal energy was calculated with the GROMACS force field using standard parameters [64]. Buried surface was calculated with WHAT IF [60]. Hydrogen-bond geometry is expressed with the WHAT IF HB2 score, ranging from 0.0 (no hydrogen bond) to 1.0 (perfect hydrogen bond), which includes information on distances and angles [60, 65]. Hydrogen bonds < 0.3 are considered to be weak and are not shown in Figures 3 and 4. Argifin/argadin atoms are identified by side chain number (see Figure 1) and standard amino acid nomenclature.

through two strong intramolecular hydrogen bonds (Table 1), forming a flat surface rich in π -electrons, interacting with the two aromatic residues that line the binding cleft (Trp137 and Phe251 in AfChiB1). On the other end of the argadin molecule, the proline side chain does not appear to make specific contacts with the protein.

Enzymology

Binding of argifin and argadin to *Serratia marcescens* chitinase B (SmChiB) was previously investigated [37],

and it was shown that argadin is a potent inhibitor with a K_i of 0.020 μM , whereas argifin is a three orders of magnitude weaker inhibitor with a K_i of 33 μM (Table 1). We have investigated the binding of these inhibitors to AfChiB1, a range of AfChiB1 mutants, and the human chitotriosidase. To conserve the (no longer available) stocks of argifin and argadin, we have used intrinsic tryptophan fluorescence as a direct approach to measuring AfChiB1 affinity rather than inhibition. Titration of increasing amounts of inhibitor leads to quenching of protein tryptophan fluorescence, which can be fitted to

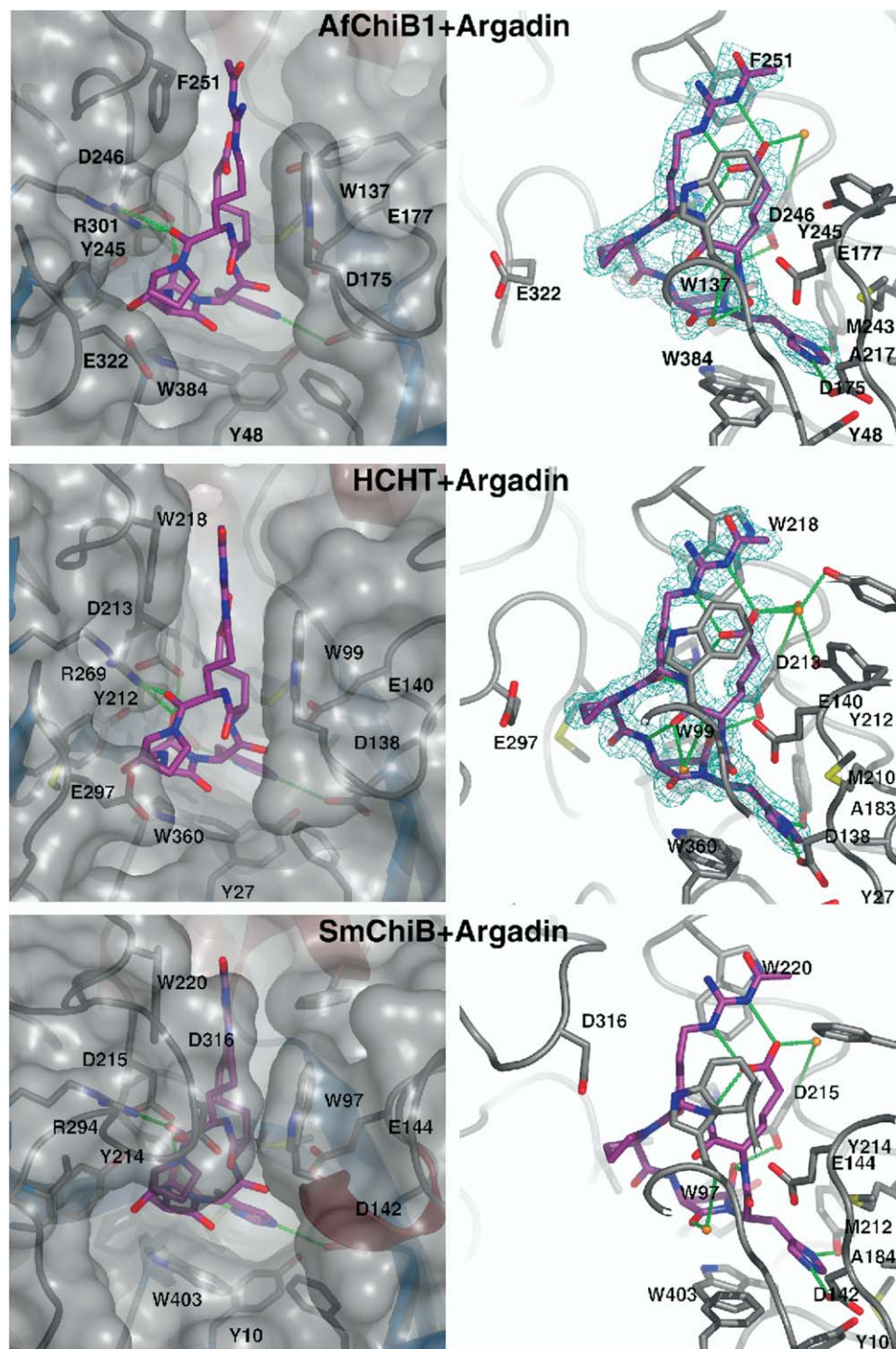


Figure 4. Comparison of Argadin Binding to Family 18 Chitinases

The crystal structures of argadin (magenta carbon atoms) in complex with AfChiB1, HCHT, and SmChiB are shown as transparent surface (left column) or sticks (right column) representations in two different orientations. Unbiased $|F_o| - |F_c|$, ϕ_{calc} electron density maps, used for building the initial inhibitor models, are shown in cyan, contoured at 2.5σ . Hydrogen bonds with a WHAT IF HB2 score > 0.3 (see Table 1) are shown as green dashed lines. Water molecules involved in water-mediated protein-ligand hydrogen bonds (Table 1) are shown as orange spheres (in the sticks images only). Protein side chains shown are those within a WHAT IF [60] contact distance of 0.75 \AA from the ligand.

a standard Langmuir binding isotherm for a single binding site, allowing the direct calculation of the dissociation constant K_d (Figure 5). Surprisingly, argifin binds

with a K_d of $0.46 \mu\text{M}$, two orders of magnitude tighter than observed for the SmChiB-argifin interaction (Table 1). Furthermore, argadin, which for SmChiB was the

Table 2. Details of Enzymology and Ligand Binding on Wild-Type and Mutant *AfChiB1*

Mutant	K_m (μM)	V_{max} ($\mu\text{M/s}$)	k_{cat} (s^{-1})	k_{cat}/K_m ($\mu\text{M}^{-1}\text{s}^{-1}$)	Argifin K_d (μM)	Argadin K_d (μM)
WT	19.9 \pm 2.8	0.0032 \pm 0.0002	1.6 \pm 0.1	0.08	0.46 \pm 0.06	0.81 \pm 0.10
D175A	ND	ND	ND	ND	3.81 \pm 0.31	3.60 \pm 0.50
E177A	ND	ND	ND	ND	ND	ND
Y245F	28.8 \pm 10.7	0.00007 \pm 0.00001	0.035 \pm 0.005	0.001	ND	5.57 \pm 0.45
D246A	16.2 \pm 8.8	0.00007 \pm 0.00001	0.035 \pm 0.005	0.002	ND	ND
R301K	34.3 \pm 7.1	0.0002 \pm 0.00002	0.1 \pm 0.01	0.003	2.16 \pm 0.09	1.02 \pm 0.55
W137A	36.4 \pm 9.6	0.0003 \pm 0.00004	0.15 \pm 0.02	0.004	ND	ND
A217G	8.4 \pm 1.8	0.0002 \pm 0.00001	0.1 \pm 0.005	0.01	4.24 \pm 1.15	2.84 \pm 0.23
M243A	31.9 \pm 6.9	0.0002 \pm 0.00002	0.1 \pm 0.01	0.003	1.73 \pm 0.21	9.39 \pm 2.04
F251A	ND	ND	ND	ND	ND	ND
T138A	10.7 \pm 1.3	0.0015 \pm 0.00006	0.75 \pm 0.03	0.07	1.21 \pm 0.13	3.04 \pm 0.80
E322A	6.3 \pm 1.1	0.0020 \pm 0.00008	1.0 \pm 0.04	0.2	1.37 \pm 0.15	2.93 \pm 0.26

All experiments were performed in triplicate, with the exception of Y245F kinetics and T138A-argadin tryptophan fluorescence, which were performed in duplicate. ND, no significant signal. The mutants are divided into three different groups, as explained in the Discussion.

tightest inhibitor of the two, binds *AfChiB1* with a K_d of only 0.81 μM , approximately 40-fold weaker compared to *SmChiB* (Table 1). To validate the tryptophan fluorescence approach, IC_{50} for argifin/argadin inhibition of *AfChiB1* were also determined (using a standard enzyme assay with 4-methylumbelliferyl-derived substrate analogs), which appeared to be similar to the K_d s derived with tryptophan fluorescence (Table 1). HCHT inhibition was also measured with standard dose-response enzyme-activity curves. Similar to the shift observed for *AfChiB1*, argifin inhibition of HCHT (IC_{50} = 4.5 μM) is increased an order of magnitude compared to *SmChiB* (Table 1). However, argadin is a low nM inhibitor of HCHT (IC_{50} = 0.013 μM), similar to *SmChiB*. The structures of the *AfChiB1*, HCHT, and *SmChiB* chitinases in complex with the inhibitors allow an interpretation of these differences in binding and inhibition. There are a number of features in the *AfChiB1*-argifin complex that explain why argifin is a 1 to 2 orders of magnitude better inhibitor for *AfChiB1* than for the other two chitinases. First, Trp384, which is conserved in all family 18 chitinases, is able to adopt a different conformation to maximize the amount of stacking with argifin's guanyl-urea moiety (Figure 3). In *AfChiB1*, 20.2 \AA^2 of this tryptophan is buried by the inhibitor, compared to 18.9 \AA^2 and 17.4 \AA^2 in the HCHT and *SmChiB* complexes, respectively. Second, *AfChiB1* is the only one of the three chitinases to make a significant hydrogen bond through the conserved Asp246 (Table 1; Figure 3) and contains the largest number of direct and water-mediated protein-inhibitor hydrogen bonds (14, compared to 9 for both the HCHT and *SmChiB* argifin complexes). The structures also explain why *SmChiB* interacts relatively poorly with argifin. Although *SmChiB* buries the largest amount of surface upon argifin binding (Table 1), it does so through a number of unfavorable interactions, which shift the inhibitor's position in the active site (Figure 3) and force it into a less favorable conformation as assessed by calculated potential energy and intramolecular hydrogen bond geometry (Table 1). *SmChiB* possesses a large loop, with Asp316 at its tip, which folds over the active site, giving it a tunnel rather than a groove character (Figure 3) [14, 30]. Asp316 is pushed into the inhibitor, with both of its terminal oxygens sterically clashing with argifin's phenyl-

alanine (distances of 2.7 and 2.9 \AA to the backbone oxygen and N-methyl group, respectively).

Analysis of the chitinase-argadin complexes also explains why argadin binds to HCHT and *SmChiB* with similar (low nM) affinity but remarkably 40-fold weaker to *AfChiB1* (Table 1). Although argadin interacts with the three chitinases through almost identical hydrogen bonds (i.e., Asp175, Tyr245, Asp246, and Arg301 in *AfChiB1*), even including two "conserved" water molecules (Figure 4; Table 1), there is a crucial difference in stacking interactions. Phe251 in *AfChiB1* (a tryptophan in HCHT and *SmChiB*; Figure 4) is unusual in that out of 208 bacterial-type family 18 chitinases available as a sequence alignment in the SMART database [38], only 10 possess a phenylalanine at this position, and the others almost without exception have a tryptophan. While this may initially seem a rather conservative substitution, there are several reports showing that the residue at this position is essential for ligand/substrate binding. Mutation of the equivalent Trp220 in *SmChiB* to alanine reduces the affinity for argifin only 12-fold, but the affinity for argadin is reduced 250-fold [37]. Similarly, mutation of this tryptophan in another chitinase shows a significant reduction in activity [32, 39]. Surface calculations with WHAT IF show that argadin stacks with 12.9 \AA^2 contact surface onto Phe251 in the *AfChiB1* complex, whereas it buries 15.0 \AA^2 and 17.7 \AA^2 on the tryptophans Trp218 and Trp220 in the HCHT and *SmChiB* complexes, respectively. It has been estimated that burial of hydrophobic surface contributes to free energy of binding with $\Delta\Delta G = 15 \text{ cal mol}^{-1} \text{ \AA}^{-2}$ [40, 41], and this does not take into account possible further favorable contributions from π - π stacking as observed here, in particular for argadin (Figure 4). Thus, the 2.1–4.8 \AA^2 extra buried surface on the tryptophans in the HCHT and *SmChiB* complexes compared to the Phe251 in *AfChiB1* could contribute to the 40-fold difference in affinity.

To further establish the contributions of individual residues to affinity and selectivity of *AfChiB1* for argifin and argadin, we have individually mutated every residue that is seen to contact either inhibitor in the complexes with *AfChiB1*, with the exception of Trp384 and Tyr48 (Figures 3 and 4). These mutants were then subjected to kinetic analyses using fluorescent substrates

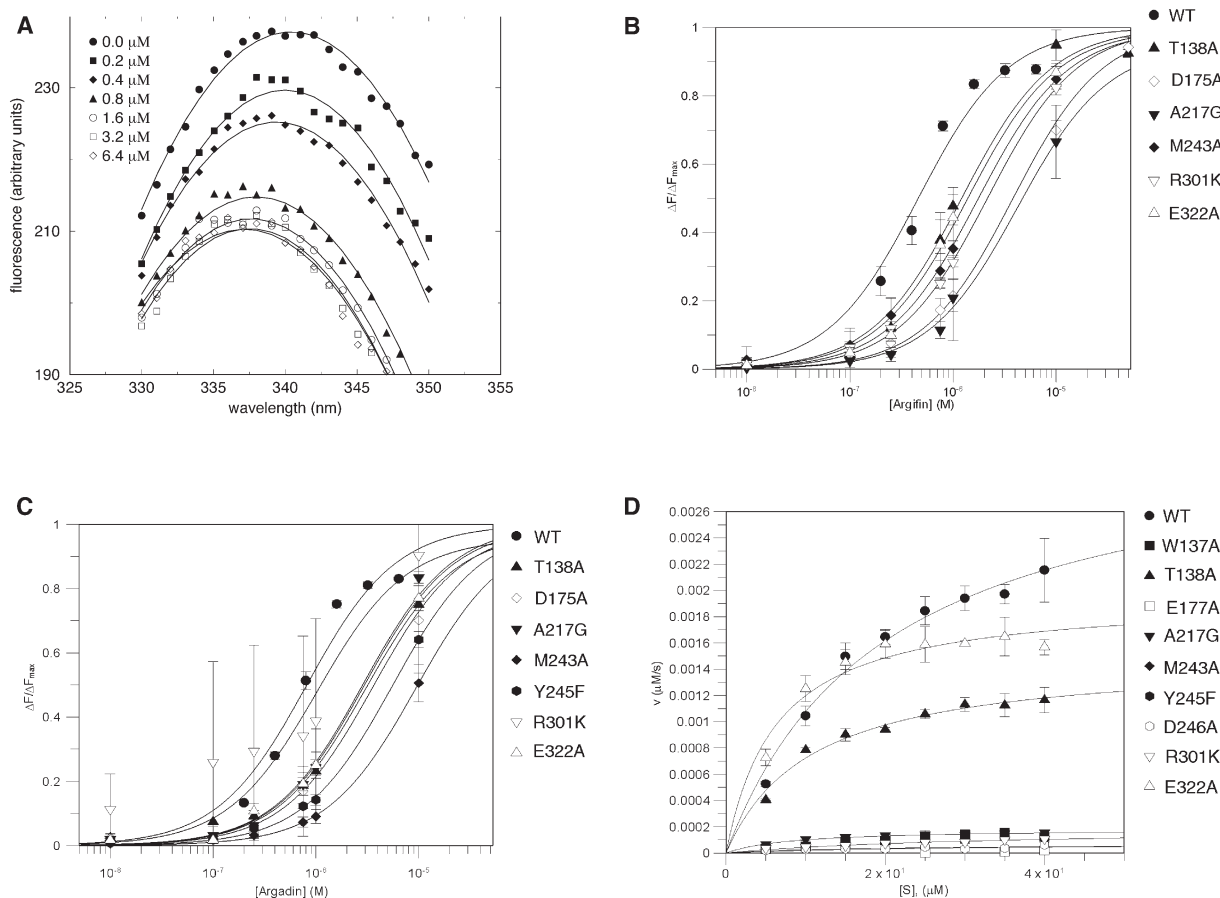


Figure 5. Kinetics and Inhibition

(A) Quenching of intrinsic AfChiB1 protein tryptophan fluorescence measured at increasing argifin concentrations. Third degree polynomials were fitted to the observed spectra. These were used to determine total fluorescence at 340 nm, plotted as fraction of maximum fluorescence in (B) and (C).

(B and C) Dose-response curves of fractional tryptophan fluorescence at 340 nm versus argifin (B) or argadin (C) concentration for wild-type and mutant AfChiB1. All data points represent the average of three measurements \pm standard deviation (except for the T138A-argadin data, which were measured in duplicate). Data were fitted against a single binding site equation $\Delta F/\Delta F_{\text{max}} = (C^*[L])/(K_d + [L])$, where C is the capacity and [L] is the ligand concentration. Calculated K_d s are shown in Table 2.

(D) Initial velocity measured at different substrate concentrations for wild-type and mutant AfChiB1. All data points represent the average of three measurements \pm standard deviation (except for the Y245F data, which were measured in duplicate). Data were fitted against the Michaelis-Menten equation $v = (V_{\text{max}}*[S])/(K_m + [S])$, with the results shown in Table 2.

and inhibitor binding experiments using tryptophan fluorescence, the results of which are shown in Table 2 and Figure 5. Based on these data and the structures of the inhibitor complexes, the mutants can be divided into three groups.

The first group concerns Asp175, Glu177, Tyr245, Asp246, and Arg301. These residues make direct hydrogen bonds to argifin/argadin (Figures 3 and 4 and Table 1) and also interact with substrate in the known chitinase-substrate complexes [13, 30, 31, 33]. Mutations of these residues reduce k_{cat} by 1 to 2 orders of magnitude, while no large effects on K_m are observed (Table 2). This suggests that these residues are crucial for catalysis rather than substrate binding, mostly in agreement with mutational studies of these residues in other family 18 chitinases [14, 15, 31, 33, 42]. Interestingly, however, there are significant effects on argifin/argadin binding (with the exception of Arg301Lys-

argadin), ranging from 4-fold reduction (Asp175Ala-argadin) to no detectable binding (Glu177, Tyr245, and Asp246). This demonstrates that all the hydrogen bonding contacts observed in the complexes make key contributions to affinity. There are two mutants that show significant differential effects on argifin versus argadin binding. While the Tyr245Phe mutation completely abrogates binding to argifin, a 7-fold reduction in affinity for argadin is observed (Table 2). Similarly, the conservative Arg301Lys substitution appears to affect argifin binding (5-fold reduction) more than argadin binding (no reduction).

The second group of mutants concerns Trp137, Ala217, Met243, and Phe251. These residues are involved in hydrophobic contacts with the substrate/reaction intermediate by stacking with the substrate (Trp137/Phe251 equivalents) or forming a pocket for the N-methylcarbamoyl group (Ala217/Met243 equivalents)

[13, 30, 31, 43]. The Trp137Ala and Phe251Ala mutations both affect substrate binding and/or k_{cat} and completely abrogate argifin/argadin binding. This is in agreement with the observation discussed earlier that Phe251 is a key factor in tuning argadin affinity. Mutations of Ala217 and Met243 have minor effects on K_{m} , but both reduce k_{cat} by an order of magnitude (Table 2). These residues are highly conserved in family 18 chitinases, and their close proximity to the C1 carbon of the substrate may well give them some involvement in stabilization of the transition state [17, 21, 30, 43]. The Ala217Gly mutation appears to specifically affect binding to argifin (9-fold reduction in K_{d}), which is seen to approach Ala217 with the terminal methyl group on the guanyl-urea moiety (Figure 3). The Met243Ala mutant mostly affects binding to argadin (12-fold reduction in K_{d}), which directly contacts the δ atom of this side chain through the face of the imidazole group of the histidine side chain (Figure 4).

The last group of mutants, Thr138Ala and Glu322Ala, involves residues that are not well conserved in family 18 chitinases. Both residues occupy a position toward the nonreducing end edge of the active site (i.e., the -2/-3 subsites) (Figures 3 and 4). Strikingly, mutation of these residues to alanine appears to slightly decrease K_{m} , while not affecting k_{cat} (Table 2). This is surprising, as both these residues have been shown to establish favorable contacts in a chitinase-substrate complex [31] and chitinase-allosamidin complexes [17, 31], including the CiCTS1-allosamidin complex [15]. However, it is worth noting that both mutations show a 3- to 4-fold reduction in K_{d} for argifin/argadin, despite the absence of specific interactions between these residues and the inhibitors. This suggests that these residues, which are not conserved in the three chitinases discussed here (Figures 3 and 4), could be worth addressing with argifin/argadin derivatives to increase selectivity of these compounds.

Discussion

The data reported here provide further insights into how two unusual natural product cyclopentapeptides inhibit family 18 chitinases through mimicry of the carbohydrate substrate. Through a combination of hydrophobic interactions and hydrogen bonding, argifin and argadin occupy the -1, +1, and +2 subsites in the active site groove of the chitinases. Although examples of structural carbohydrate mimicry through peptide molecules has been reported previously, these have so far involved inactive proteins (e.g., antibodies [44–46]) or glycosidases bound to macromolecular inhibitors (e.g., amylase with a lectin-like inhibitor [47]). Argifin and argadin are the first examples of low-molecular-weight peptide inhibitors that act on a carbohydrate-processing enzyme.

There are a number of family 18 chitinases of the bacterial class whose function is not well understood, yet there is evidence that they are interesting targets for inhibition with selective compounds from a chemotherapeutic perspective. These chitinases include those from (parasitic) nematodes [48–51], protozoan parasites [7–9], insects [52], and mammals [3, 10]. Although allo-

samidin does inhibit this class of chitinases [12], it only addresses the -1 (catalytic) subsite through its allosamidin moiety and the -2/-3 subsites with the N-acetyl allosamine sugars [13, 15–17, 30]. The structural and biochemical data presented here demonstrate that the +1/+2 subsites, lined by two aromatics (Trp137 and Phe251 in AfChiB1; Figures 3 and 4), are, along with the -1 subsite, the main determinants for argifin/argadin affinity and selectivity. It should be noted that the family 18 chitinases of the plant class have a significantly smaller catalytic core and completely lack the loops that carry these aromatic residues in the larger bacterial-class chitinases. In the light of the chitinase-argifin/argadin structures and mutagenesis presented here, it is therefore likely that the plant-class family 18 chitinases are not inhibited by these cyclopentapeptides, whereas they are potently inhibited by allosamidin [12, 13]. Indeed, initial inhibition tests with argadin against *SmChiC*, a plant-class family 18 chitinase from *S. marcescens*, have shown no significant inhibition at up to 50 μM concentration (V.G.H. Eijsink, personal communication).

The comparison of the chitinase-argifin/argadin complexes shows that although there is high sequence conservation of the residues in the active site, and the majority of protein-inhibitor contacts are made through these residues, subtle changes in residues near the active site can have significant effects. It should be possible to exploit these subtle differences (e.g., the residues at positions 138, 251, and 322 AfChiB1) to design argifin/argadin derivatives that specifically inhibit a particular chitinase of the bacterial class. Such molecules could be tools to study the complex functions of chitinases in fungi, nematodes, protozoan parasites, insects, and mammals. Total synthesis of argifin and argadin is currently being explored to overcome the limited availability of these compounds from natural sources, and we hope to report on the design and synthesis of such derivatives in the near future.

Significance

Family 18 chitinases are enzymes that hydrolyze the glycosidic bonds of chitin, a polymer of $\beta(1,4)$ -linked N-acetyl glucosamine, which is found as a component of the fungal cell wall, insect exoskeleton, and nematode egg shell. Inhibitors of these enzymes are of considerable interest as research tools but also may have chemotherapeutic potential against pathogenic fungi, insects, and nematodes. Here, we show how two natural product cyclopentapeptides, argifin and argadin, inhibit chitinases by binding to the active site, mimicking interactions that these enzymes make with their natural substrate, chitin. The crystal structures of complexes of chitinases with argifin/argadin together with binding studies on a range of mutants show how these remarkable peptides mimic the shape, hydrogen bonding patterns, and hydrophobic stacking of the substrate. There appear to be interesting differences in the details of these interactions between a chitinase from the fungal pathogen *Aspergil-*

Ius fumigatus and a human chitinase, which may allow the development of specific inhibitors.

Experimental Procedures

Cloning

A fragment corresponding to AfChiB1 was amplified by PCR from the previously described gene [53] (GeneBank accession no. AY217660) in pPICZ α A as a template (forward primer, 5'-GGATC CAGCTCCGGTTATCGCTCGGTC-3'; reverse primer, 5'-CCTAGGTT AGGTTTGCATGCCATTGCGCAG-3'). The PCR product was ligated into pCR 2.1-TOPO (Invitrogen) and subcloned into the pGEX-6P-1 vector (Amersham) using the BamH1 and EcoR1 restriction sites (indicated in bold above). Single amino acid residue changes were made using the Quick Change Site Directed Mutagenesis Kit (Stratagene) following the manufacturer's instructions. All plasmids were verified by DNA sequencing (The Sequencing Service, School of Life Sciences, University of Dundee, Scotland, UK).

Expression and Purification

The AfChiB1-pGEX-6P-1 construct was transformed into *E. coli* BL21(DE3) pLysS cells. Cells were grown overnight in Luria-Bertani medium (LB)+ ampicillin (100 μ g/ml). From this culture, 10 ml of cells were used to inoculate 1 liter of LB media. The cells were grown to OD₆₀₀ = 0.5 before protein expression was induced by the addition of 250 μ M isopropyl- β -D-thiogalactopyranoside, and then the cells were cultured for an additional 4 hr at 37°C. The cells were harvested by centrifugation at 2500 g for 30 min, flash frozen in liquid nitrogen, thawed at 37°C, and resuspended in 25 ml of lysis buffer (50 mM HEPES, 250 mM NaCl [pH 7.5]) and half a "Complete" protease inhibitor tablet (Roche). Lysis was achieved by the addition of 20 μ l DNase (Roche) (10 u/ μ l) and approximately 13 mg lysozyme (Sigma) incubating for 10 min on ice, followed by 4 \times 30 s sonication. The lysate was centrifuged at 18,900 g for 30 min and passed through a 0.45 μ m filter. The filtrate was then incubated at 4°C on a rotating platform with 2 ml glutathione-Sepharose beads (Amersham) prewashed with lysis buffer for 2 hr. The N-terminal GST tag was removed from the GST-AfChiB1 fusion protein by incubating the beads with PreScission Protease (50 μ g) at 4°C for 18 hr. The supernatant of the beads and a subsequent wash were filtered to remove traces of beads, concentrated to 4 ml, and loaded onto a Superdex 75, 26/60 gel filtration column preequilibrated in buffer (25 mM HEPES, 250 mM NaCl [pH 7.5]). The pure fractions were verified by SDS-PAGE and pooled and then dialyzed overnight into 50 mM Tris (pH 8.0) at 4°C.

Crystallization and Structure Determination

Pure AfChiB1 protein was spin concentrated to 28 mg/ml. Vapor diffusion crystallization experiments were set up by mixing 1 μ l of protein and 1 μ l of mother liquor consisting of 0.1 M Tris/HCl (pH 9.5) and 1.4 M Li₂SO₄ and equilibrated against a reservoir containing 0.5 ml of mother liquor. Rod-shaped crystals appeared after 3 days growing to a maximum size of 0.3 \times 0.1 \times 0.1 mm. Crystals used for soaking experiments were washed three times in 0.1 M sodium citrate (pH 5.5) and 1.4 M Li₂SO₄, with the final drop containing approximately 60-fold molar excess of ligand, using 30 min soaking time. The crystals were cryoprotected by a 10 s immersion in 3 M Li₂SO₄ and then frozen in a nitrogen cryostream for data collection.

Human chitotriosidase was purified and prepared for crystallization as described previously [3, 28, 54]. Hanging drop vapor diffusion in 1 ml wells was used to cocrystallise complexes of HCHT with argifin and argadin. Plate-shaped crystals formed of approximate dimensions 0.2 \times 0.2 \times 0.05 mm in a 1 μ l drop containing 4 mg/ml HCHT, 100-fold excess ligand, 10% isopropanol, 10% PEG 4000, and 0.05 M sodium citrate (pH 5.6). The crystals were transferred to a 0.25 μ l drop of mother liquor in which the concentration of isopropanol had been increased to 50% for cryoprotection before freezing in a 100 K nitrogen cryostream.

Data were collected on beamline BM14 at the European Synchrotron Radiation Facility (Grenoble, France) and beamline X11 at the Deutsches Elektronen Synchrotron (Hamburg, Germany). Dif-

fraction data were processed with the HKL suite of programs [55] (Table S1).

The native AfChiB1 structure was solved by molecular replacement with AMoRe [56] using the *C. immitis* chitinase 1 (Protein Data Bank [PDB] code 1D2K) as a search model [27]. With two molecules in the asymmetric unit, a clear solution was obtained, which gave an R factor of 0.27 with 3.0 Å data after rigid body refinement in CNS [57]. This was used as a starting structure for the refinement of the other complexes. The HCHT-argifin complex, which crystallized in a different space group from native HCHT, was solved by molecular replacement with AMoRe [56] using the native structure as a search model (PDB code 1GUV [28]). A clear solution was obtained (R = 0.323, correlation coefficient = 71.6) for a single molecule in the asymmetric unit.

All refinement was initiated by rigid body refinement, followed by simulated annealing with CNS [57], followed by iterative cycles of refinement and model binding in O [58]. Models for the ligands were not included until their conformations were well defined by the unbiased $|F_o| - |F_c|$, ϕ_{calc} electron density maps (Figures 2B, 3, and 4). Ligand starting structures and topologies were generated with PRODRG [59]. Further refinement resulted in the final models described in Table S1. In the interest of simplicity, differences between the complexes are discussed using the first monomer in the coordinate files.

Structural superpositions were performed with the MOTIF module of WHAT IF [60] and LSQKAB from the CCP4 package [61]. Images were generated with PYMOL (<http://pymol.sourceforge.net/>).

Enzymology

Binding of ligands to wild-type and mutant AfChiB1 was analyzed by ligand-induced quenching of intrinsic tryptophan fluorescence. Fluorescence measurements were carried out with a Varian Cary Eclipse fluorescence spectrophotometer equipped with a thermostatted cuvette holder equilibrated at 25°C. Emission spectra were recorded from 330–360 nm upon excitation at 295 nm. Excitation and emission slits were opened to 10 nm and 20 nm, respectively, and the spectra were recorded at a scan speed of 9–60 nm/min. Standard reaction mixtures contained 0.5 μ M of AfChiB1 in 50 mM sodium citrate, 250 mM sodium chloride (pH 5.5) to a final volume of 1 ml. After preincubation for 10 min at 25°C within the cuvette holder, aliquots of argifin or argadin were added to the mixture (final volume did not exceed 5% of the total volume). The emission spectrum was recorded after each addition following mixing and 5 min incubation. All of the spectra were corrected for the background emission signal from both the buffer and the unbound ligand and repeated in triplicate. The equilibrium dissociation constant could be obtained from fitting the fractional fluorescence intensity data to a single site binding equation using nonlinear regression analysis with the software GraFit [62].

Michaelis-Menten parameters of wild-type and mutant AfChiB1 were determined using the fluorogenic substrate 4-methylumbelliferyl β -D-N,N'-diacetylchitobiose (4MU-NAG2; Sigma). Standard reaction mixtures contained 2 nM of AfChiB1, 0.1 mg/ml BSA, and 5–40 μ M of the fluorogenic substrate in McIlvain buffer (100 mM citric acid, 200 mM sodium phosphate [pH 5.5]) to a final volume of 50 μ l. Reaction mixtures were incubated for 10 min at 37°C, after which the reaction was stopped with the addition of 25 μ l of 3 M glycine-NaOH (pH 10.3). The fluorescence of the released 4-methylumbelliferone was quantified using a FLx 800 microtitreplate fluorescence reader (Bio-Tek Instruments Inc.) (excitation 366 nm, emission 445 nm). Experiments were performed in triplicate. Production of 4-methylumbelliferone was linear with time for the incubation period used, and less than 10% of available substrate was hydrolyzed. The IC₅₀s of argifin/argadin against AfChiB1 were determined using the same protocol but with a constant substrate concentration of 20 μ M and 0.01–100 μ M inhibitor.

The IC₅₀s of argifin/argadin against the human chitinase were determined using the fluorogenic substrate 4-methylumbelliferyl- β -D-N,N',N''-triacetylchitotriose (4MU-NAG3, Sigma, St Louis, MO) in a standard assay, as previously described [3]. Briefly, in a final volume of 125 μ l, a constant amount of enzyme was incubated with 0.022 mM substrate in McIlvain buffer (adjusted to pH 5.2)

containing 1 mg/ml BSA for 20 min at 37°C in the presence of different concentrations of inhibitor. After addition of 2.5 ml 0.3 M glycine-NaOH (pH 10.6), the fluorescence of the liberated 4MU was quantified using a Perkin Elmer LS2 fluorimeter (excitation 366 nm, emission 445 nm). The ability of chitotriosidase to transglycosylate does not allow determination of K_i values [63].

Supplemental Data

A table with details of data collection and structure refinement is available online at <http://www.chembiol.com/cgi/content/full/12/1/65/DC1/>.

Accession Numbers

The coordinates and structure factors have been deposited in the PDB under ID codes 1W9P (native AfChiB1), 1WAV (AfChiB1 + argadin), 1W9V (AfChiB1 + argifin), 1WAW (HCHT + argadin), and 1WB0 (HCHT + argifin).

Acknowledgments

We thank the European Synchrotron Radiation Facility, Grenoble and the Deutsches Elektronen Synchrotron (Hamburg, Germany) for the time at beamlines BM14 and X11, respectively. D.V.A. is supported by a Wellcome Trust Senior Research Fellowship. D.J.A. was supported by the Wellcome Trust. D.R.H. is supported by a BBSRC CASE studentship together with Cyclacel. F.V.R. is supported by a BBSRC CASE studentship together with Syngenta. We thank Vincent Eijsink and Ian Eggleston for critically reading the manuscript and useful discussions and Alex Jaques and Mariam Taib for their help in preparation of recombinant AfChiB1.

Received: September 6, 2004

Revised: October 7, 2004

Accepted: October 14, 2004

Published: January 21, 2005

References

1. Brurberg, M.B., Nes, I.F., and Eijsink, V.G.H. (1996). Comparative studies of chitinases A and B from *Serratia marcescens*. *Microbiol.* **142**, 1581–1589.
2. Hollak, C.E.M., van Weely, S., van Oers, M.H.J., and Aerts, J.M.F.G. (1994). Marked elevation of plasma chitotriosidase activity - a novel hallmark of Gaucher disease. *J. Clin. Invest.* **93**, 1288–1292.
3. Boot, R.G., Renkema, G.H., Verhoek, M., Strijland, A., Bliet, J., de Meulemeester, T.M.A.M.O., Mannens, M.M.A.M., and Aerts, J.M.F.G. (1998). The human chitotriosidase gene—nature of inherited enzyme deficiency. *J. Biol. Chem.* **273**, 25680–25685.
4. Takaya, N., Yamazaki, D., Horiuchi, H., Ohta, A., and Takagi, M. (1998). Cloning and characterisation of a chitinase-encoding gene *chiA* from *Aspergillus nidulans*, disruption of which decreases germination frequency and hyphal growth. *Biosci. Biotechnol. Biochem.* **62**, 60–65.
5. Shiomi, K., Arai, N., Iwai, Y., Turberg, A., Koelbl, H., and Omura, S. (2000). Structure of argifin, a new chitinase inhibitor produced by *Gliocladium* sp. *Tetrahedron Lett.* **41**, 2141–2143.
6. Arai, N., Shiomi, K., Yamaguchi, Y., Masuma, R., Iwai, Y., Turberg, A., Koelbl, H., and Omura, S. (2000). Argadin, a new chitinase inhibitor, produced by *Clonostachys* sp. FO-7314. *Chem. Pharm. Bull. (Tokyo)* **48**, 1442–1446.
7. Vinetz, J.M., Dave, S.K., Specht, C.A., Brameld, K.A., Xu, B., Hayward, R., and Fidock, D.A. (1999). The chitinase PfCht1 from the human malaria parasite *Plasmodium falciparum* lacks proenzyme and chitin-binding domains and displays unique substrate preferences. *Proc. Natl. Acad. Sci. USA* **96**, 14061–14066.
8. Vinetz, J.M., Valenzuela, J.G., Specht, C.A., Aravind, L., Langer, R.C., Ribeiro, J.M., and Kaslow, D.C. (2000). Chitinases of the avian malaria parasite *Plasmodium gallinaceum*, a class of enzymes necessary for parasite invasion of the mosquito midgut. *J. Biol. Chem.* **275**, 10331–10341.
9. Tsai, Y.-L., Hayward, R.E., Langer, R.C., Fidock, D.A., and Vinetz, J.M. (2001). Disruption of *Plasmodium falciparum* chitinase markedly impairs parasite invasion of mosquito midgut. *Infect. Immun.* **69**, 4048–4054.
10. Zhu, Z., Zheng, T., Homer, R.J., Kim, Y.K., Chen, N.Y., Cohn, L., Hamid, Q., and Elias, J.A. (2004). Acidic mammalian chitinase in asthmatic Th2 inflammation and IL-13 pathway activation. *Science* **304**, 1678–1682.
11. Sakuda, S., Isogai, A., Matsumoto, S., Suzuki, A., and Koseki, K. (1986). The structure of allosamidin, a novel insect chitinase inhibitor produced by *Streptomyces* sp. *Tetrahedron Lett.* **27**, 2475–2478.
12. Sakuda, S. (1996). Studies on the chitinase inhibitors, allosamidins. In *Chitin Enzymology*, Volume Two, R.A.A. Muzzarelli, ed. (Italy: Atec Edizioni), pp. 203–212.
13. Terwisscha van Scheltinga, A.C., Kalk, K.H., Beintema, J.J., and Dijkstra, B.W. (1994). Crystal-structures of hevamine, a plant defense protein with chitinase and lysozyme activity, and its complex with an inhibitor. *Structure* **2**, 1181–1189.
14. van Aalten, D.M.F., Synstad, B., Brurberg, M.B., Hough, E., Rise, B.W., Eijsink, V.G.H., and Wierenga, R.K. (2000). Structure of a two-domain chitotriosidase from *Serratia marcescens* at 1.9 Å resolution. *Proc. Natl. Acad. Sci. USA* **97**, 5842–5847.
15. Bortone, K., Monzingo, A.F., Ernst, S., and Robertus, J.D. (2002). The structure of an allosamidin complex with the *Coccidioides immitis* chitinase defines a role for a second acid residue in substrate-assisted mechanism. *J. Mol. Biol.* **320**, 293–302.
16. Papanikolaou, Y., Tavlas, G., Vorgias, C.E., and Petratos, K. (2003). De novo purification scheme and crystallization conditions yield high-resolution structures of chitinase A and its complex with the inhibitor allosamidin. *Acta Crystallogr. D Biol. Crystallogr.* **59**, 400–403.
17. Rao, F.V., Houston, D.R., Boot, R.G., Aerts, J.M.F.G., Sakuda, S., and van Aalten, D.M.F. (2003). Crystal structures of allosamidin derivatives in complex with human macrophage chitinase. *J. Biol. Chem.* **278**, 20110–20116.
18. Berecibar, A., Grandjean, C., and Siriwardena, A. (1999). Synthesis and biological activity of natural aminocyclopentitol glycosidase inhibitors: mannosidins, trehalosins, allosamidins and their analogues. *Chem. Rev.* **99**, 779–844.
19. Izumida, H., Imamura, N., and Sano, H. (1996). A novel chitinase inhibitor from a marine bacterium *Pseudomonas* sp. *J. Antibiot. (Tokyo)* **49**, 76–80.
20. Takadera, T., Nomoto, A., Izumida, H., Nishijima, M., and Sano, H. (1996). The effect of chitinase inhibitors, cyclo(Arg-Pro) against cell separation of *Saccharomyces cerevisiae* and the morphological change of *Candida albicans*. *J. Antibiot. (Tokyo)* **49**, 829–831.
21. Houston, D.R., Eggleston, I., Synstad, B., Eijsink, V.G.H., and van Aalten, D.M.F. (2002). The cyclic dipeptide Cl-4 inhibits family 18 chitinases by structural mimicry of a reaction intermediate. *Biochem. J.* **368**, 23–27.
22. Houston, D.R., Synstad, B., Eijsink, V.G.H., Stark, M.J.R., Eggleston, I., and van Aalten, D.M.F. (2004). Structure-based exploration of cyclic dipeptide chitinase inhibitors. *J. Med. Chem.* **47**, 5713–5720.
23. Davies, G., and Henrissat, B. (1995). Structures and mechanisms of glycosyl hydrolases. *Structure* **3**, 853–859.
24. Pishko, E.J., Kirkland, T.N., and Cole, G.T. (1995). Isolation and characterization of two chitinase-encoding genes (*cts1*, *cts2*) from the fungus *Coccidioides immitis*. *Gene* **167**, 173–177.
25. Perrakis, A., Tews, I., Dauter, Z., Oppenheim, A.B., Chet, I., Wilson, K.S., and Vorgias, C.E. (1994). Crystal structure of a bacterial chitinase at 2.3 Å resolution. *Structure* **2**, 1169–1180.
26. Escott, G.M., Hearn, V.M., and Adams, D.J. (1998). Inducible chitinolytic system of *Aspergillus fumigatus*. *Microbiology* **144**, 1575–1581.
27. Hollis, T., Mozingo, A.F., Bortone, K., and Ernst, S. (2000). Rebecca Cox, and J. D. Robertus, The X-ray structure of a chitinase from the pathogenic fungus *Coccidioides immitis*. *Protein Sci.* **9**, 544–551.
28. Fusetti, F., von Moeller, H., Houston, D., Rozeboom, H.J., Dijkstra, B.W., Boot, R.G., Aerts, J.M.F.G., and van Aalten, D.M.F.

- (2002). Structure of human chitotriosidase—implications for specific inhibitor design and function of mammalian chitinase-like lectins. *J. Biol. Chem.* **277**, 25537–25544.
29. Houston, D.R., Recklies, A.D., Krupa, J.C., and van Aalten, D.M.F. (2003). Structure and ligand-induced conformational change of the 39 kD glycoprotein from human articular chondrocytes. *J. Biol. Chem.* **278**, 30206–30212.
 30. van Aalten, D.M.F., Komander, D., Synstad, B., Gåseidnes, S., Peter, M.G., and Eijsink, V.G.H. (2001). Structural insights into the catalytic mechanism of a family 18 exo-chitinase. *Proc. Natl. Acad. Sci. USA* **98**, 8979–8984.
 31. Papanikolaou, Y., Prag, G., Tavlas, G., Vorgias, C.E., Oppenheim, A.B., and Petratos, K. (2001). High resolution structural analyses of mutant chitinase A complexes with substrates provide new insight into the mechanism of catalysis. *Biochemistry* **40**, 11338–11343.
 32. Uchiyama, T., Katouno, F., Nikaidou, N., Nonaka, T., Sugiyama, J., and Watanabe, T. (2001). Roles of the exposed aromatic residues in crystalline chitin hydrolysis by chitinase a from *Serratia marcescens* 2170. *J. Biol. Chem.* **276**, 41343–41349.
 33. Bokma, E., Rozeboom, H.J., Sibbald, M., Dijkstra, B.W., and Beintema, J.J. (2002). Expression and characterization of active site mutants of hevamine, a chitinase from the rubber tree *Hevea brasiliensis*. *Eur. J. Biochem.* **269**, 893–901.
 34. James, J.A., and Lee, B.H. (1996). Characterization of glucosylase from *Lactobacillus amylovorus* ATCC 33621. *Biotechnol. Lett.* **18**, 1401–1406.
 35. Kimura, A., Takata, M., Fukushi, Y., Mori, H., Matsui, H., and Chiba, S. (1997). A catalytic amino acid and primary structure of active site in *Aspergillus niger* alpha-glucosidase. *Biosci. Biotechnol. Biochem.* **67**, 1091–1098.
 36. Sabin, E., Schubert, H., Murshudov, G., Wilson, K.S., Siika-Aho, M., and Penttila, M. (2000). The three-dimensional structure of a *Trichoderma reesei* beta-mannanase from glycoside hydrolase family 5. *Acta Crystallogr. D Biol. Crystallogr.* **56**, 3–13.
 37. Houston, D.R., Shiomi, K., Arai, N., Omura, S., Peter, M.G., Turberg, A., Synstad, B., Eijsink, V.G.H., and van Aalten, D.M.F. (2002). High-resolution structures of a chitinase complexed with natural product cyclopentapeptide inhibitors: Mimicry of carbohydrate substrate. *Proc. Natl. Acad. Sci. USA* **99**, 9127–9132.
 38. Letunic, I., Copley, R.R., Schmidt, S., Ciccarelli, F.D., Doerks, T., Schultz, J., Ponting, C.P., and Bork, P. (2004). SMART 4.0: towards genomic data integration. *Nucleic Acids Res.* **32**, D142–D144.
 39. Watanabe, T., Ariga, Y., Sato, U., Toratani, T., Hashimoto, M., Nikaidou, N., Kezuka, Y., Nonaka, T., and Sugiyama, J. (2003). Aromatic residues within the substrate-binding cleft of *Bacillus circulans* chitinase A1 are essential for hydrolysis of crystalline chitin. *Biochem. J.* **376**, 237–244.
 40. Eisenberg, D., and McLachlan, A.D. (1986). Solvation energy in protein folding and binding. *Nature* **319**, 199–203.
 41. Vallone, B., Miele, A.E., Vecchini, P., Chiancone, E., and Brunori, M. (1998). Free energy of burying hydrophobic residues in the interface between protein subunits. *Proc. Natl. Acad. Sci. USA* **95**, 6103–6107.
 42. Prag, G., Papanikolaou, Y., Tavlas, G., Vorgias, C.E., Petratos, K., and Oppenheim, A.B. (2000). Structures of chitinase mutants complexed with the substrate di-N-acetyl-D-glucosamine: the catalytic role of the conserved acidic pair, aspartate 539 and glutamate 540. *J. Mol. Biol.* **300**, 611–617.
 43. Tews, I., Terwisscha van Scheltinga, A.C., Perrakis, A., Wilson, K.S., and Dijkstra, B.W. (1997). Substrate-assisted catalysis unifies two families of chitinolytic enzymes. *J. Am. Chem. Soc.* **119**, 7954–7959.
 44. Desmyter, A., Transue, T.R., Ghahroudi, M.A., Thi, M.H.D., Poortmans, F., Hamers, R., Muyldermans, S., and Wyns, L. (1996). Crystal structure of a camel single-domain V-H antibody fragment in complex with lysozyme. *Nat. Struct. Biol.* **3**, 803–811.
 45. Transue, T.R., De Genst, E., Ghahroudi, M.A., Wyns, L., and Muyldermans, S. (1998). Camel single-domain antibody inhibits enzyme by mimicking carbohydrate substrate. *Proteins* **32**, 515–522.
 46. Vyas, N.K., Vyas, M.N., Chervenak, M.C., Bundle, D.R., Pinto, B.M., and Quioco, F.A. (2003). Structural basis of peptide-carbohydrate mimicry in an antibody-combining site. *Proc. Natl. Acad. Sci. USA* **100**, 15023–15028.
 47. Bompard-Gilles, C., Rousseau, P., Rouge, P., and Payan, F. (1996). Substrate mimicry in the active center of a mammalian alpha-amylase: Structural analysis of an enzyme-inhibitor complex. *Structure* **4**, 1441–1452.
 48. Gooday, G.W., Brydon, L.J., and Chappell, L.H. (1988). Chitinase in female *Onchocerca gibsoni* and its inhibition by allosamidin. *Mol. Biochem. Parasitol.* **29**, 223–225.
 49. Arnold, K., Brydon, L.J., Chappell, L.H., and Gooday, G.W. (1993). Chitinolytic activities in heligmosomoides-polygyrus and their role in egg hatching. *Mol. Biochem. Parasitol.* **58**, 317–323.
 50. Adam, R., Kaltmann, B., Rudin, W., Friedrich, T., Marti, T., and Lucius, R. (1996). Identification of chitinase as the immunodominant filarial antigen recognized by sera of vaccinated rodents. *J. Biol. Chem.* **271**, 1441–1447.
 51. Wu, Y., Egerton, G., Underwood, A.P., Sakuda, S., and Bianco, A.E. (2001). Expression and secretion of a larval-specific chitinase (family 18 glycosyl hydrolase) by the infective stages of the parasitic nematode, *Onchocerca volvulus*. *J. Biol. Chem.* **276**, 42557–42564.
 52. Cohen, E. (1993). Chitin synthesis and degradation as targets for pesticide action. *Arch. Insect Biochem. Physiol.* **22**, 245–261.
 53. Jaques, A.K., Fukamizo, T., Hall, D., Barton, R.C., Escott, G.M., Parkinson, T., Hitchcock, C.A., and Adams, D.J. (2003). Disruption of the gene encoding the ChiB1 chitinase of *Aspergillus fumigatus* and characterization of a recombinant gene product. *Microbiology* **149**, 2931–2939.
 54. Funk, W.D., MacGillivray, R.T.A., Mason, A.B., Brown, S.A., and Woodworth, R.C. (1990). Expression of the amino-terminal half-molecule of human serum transferrin in cultured-cells and characterization of the recombinant protein. *Biochemistry* **29**, 1654–1660.
 55. Otwinowski, Z., and Minor, W. (1997). Processing of X-ray diffraction data collected in oscillation mode. *Methods Enzymol.* **276**, 307–326.
 56. Navaza, J. (1994). AMoRe: an automated package for molecular replacement. *Acta Crystallogr. A* **50**, 157–163.
 57. Brunger, A.T., Adams, P.D., Clore, G.M., Gros, P., Gross-Kunstleve, R.W., Jiang, J.-S., Kuszewski, J., Nilges, M., Pannu, N.S., Read, R.J., et al. (1998). Crystallography and NMR system: a new software system for macromolecular structure determination. *Acta Crystallogr. D Biol. Crystallogr.* **54**, 905–921.
 58. Jones, T.A., Zou, J.Y., Cowan, S.W., and Kjeldgaard, M. (1991). Improved methods for building protein models in electron density maps and the location of errors in these models. *Acta Crystallogr. A* **47**, 110–119.
 59. Schuettelkopf, A.W., and van Aalten, D.M.F. (2004). PRODRG: a tool for high-throughput crystallography of protein-ligand complexes. *Acta Crystallogr. D Biol. Crystallogr.* **60**, 1355–1363.
 60. Vriend, G. (1990). WHAT IF: a molecular modeling and drug design program. *J. Mol. Graph.* **8**, 52–56.
 61. CCP4 (Collaborative Computational Project, Number 4)(1994). The CCP4 suite: programs for protein crystallography. *Acta Crystallogr. D Biol. Crystallogr.* **50**, 760–763.
 62. Leatherbarrow, R.J. (2001). GraFit Version (Horley, UK: Erithacus Software Ltd.).
 63. Aguilera, B., Ghaharali-van der Lugt, K., Helmond, M.T.J., Out, J.M.M., Donker-Koopman, W.E., Groener, J.E.M., Boot, R.G., Renkema, G.H., van der Marel, G.A., van Boom, J.H., et al. (2003). Transglycosidase activity of chitotriosidase—improved enzymatic assay for the human macrophage chitinase. *J. Biol. Chem.* **278**, 40911–40916.
 64. van der Spoel, D., Lindahl, E., Hess, B., van Buuren, A.R., Apol, E., Meulenhoff, P.J., Tieleman, D.P., Sijbers, A.L.T.M., Feenstra, K.A., van Drunen, R., and Berendsen, H.J.C. (2004).
 65. Hooft, R.W.W., Sander, C., and Vriend, G. (1996). Positioning hydrogen atoms by optimizing hydrogen-bond networks in protein structures. *Proteins* **26**, 363–376.